

Repository Istituzionale dei Prodotti della Ricerca del Politecnico di Bari

On the Energy Impact of Urban Heat Island in Sydney. Climate and Energy Potential of Mitigation Technologies

This is a post print of the following article

Original Citation:
On the Energy Impact of Urban Heat Island in Sydney. Climate and Energy Potential of Mitigation Technologies / Santamouris, M., Haddad, S., Saliari, M., Vasilakopoulou, K., Synnefa, A., Paolini, R., Ulpiani, G., Garshasbi, S., Fiorito, F.. - In: ENERGY AND BUILDINGS. - ISSN 0378-7788. - ELETTRONICO. - 166:(2018), pp. 154-164. [10.1016/j.enbuild.2018.02.007]

Availability:
This version is available at http://hdl.handle.net/11589/122669 since: 2021-03-06

Published version
DOI:10.1016/j.enbuild.2018.02.007

Publisher:

Terms of use:

(Article begins on next page)

17 November 2026

On the Energy Impact of Urban Heat Island in Sydney. Climate and Energy Potential of Mitigation Technologies

Mattheos Santamouris [a], Shamila Haddad [a], Maria Saliari [b], Konstantina Vasilakopoulou [a], Afroditi Synnefa [a], Riccardo Paolini [a], Giulia Ulpiani [a,c], Samira Garshasbi [a] , Francesco Fiorito [a,d,*]

[a] Faculty of Built Environment, University of New South Wales, Sydney, Australia; m.santamouris@unsw.edu.au (M.S.), s.haddad@unsw.edu.au (S.H.), f.fiorito@unsw.edu.au (F.F.), k.vasilakopoulou@unsw.edu.au (K.V.), a.synnefa@unsw.edu.au (A.S.), r.paolini@unsw.edu.au (R.P.), g.ulpiani@unsw.edu.au (G.U.), s.garshasbi@unsw.edu.au (S.G.)

[b] Department of Physics, National and Kapodistrian University of Athens, Athens, Greece; msaliari@phys.uoa.gr

[c] Department of Industrial Engineering and Mathematical Sciences (DIISM), Polytechnic University of Marche, Ancona, Italy; g.ulpiani@pm.univpm.it

[d] Department of Civil, Environmental, Land, Building Engineering and Chemistry (DICATECh), Polytechnic University of Bari, Bari, Italy; francesco.fiorito@poliba.it

* Corresponding author. E-mail: francesco.fiorito@poliba.it. Tel: +39 080 5963401

Abstract

Urban Heat Island (UHI) is a phenomenon resulting in the increase of ambient temperature in dense areas of cities in comparison with rural areas. UHI has been demonstrated to be relevant in the Sydney metropolitan area, with a peak intensity of up to 6 °C. This has the consequence of increasing of up to three times the cooling demand of buildings. With the general aim of mitigating the effects of UHI in Sydney, several strategies, involving the use of outdoor surfaces with high Solar Reflectance and the use of greenery on outdoor surfaces at ground level and on roofs have been implemented and tested. Moreover, the benefits due to the adoption of mitigation technologies, in terms of reducing both UHI intensity and building cooling demand have been predicted. Results have shown that solutions involving the increase of the global albedo of the city demonstrate the highest benefits, achieving a reduction of peak ambient temperature of up to 3°C and of peak cooling demand of residential buildings of up to 20%.

Keywords: *Urban Heat Island; Mitigation Technologies; Building Energy Demand; Residential Buildings; Albedo; Green Roofs, Greenery.*

1. Introduction

Urban Heat Island (UHI) is a well-recognized and documented phenomenon affecting cities [1-6]. UHI develops in conjunction with climate change, resulting in an even greater increase of hot periods in urban areas than in their rural corresponding parts [7]. Studies performed in the last three decades have demonstrated a worldwide spread of the phenomenon. In Europe, the average maximum UHI intensity recorded was between 0.3 °C and 6.8 °C (average of 2.6 °C), with absolute maximum peaks close to 12 °C [8, 9]. Similarly, studies performed in Asian and Australian cities have shown how UHI phenomenon is significant, with intensities varying between 0.4 °C and 11 °C [10].

UHI has an important effect on pollution [11], and on human health [12-16]. Baccini et al. [12], analysing the relationship between maximum daily apparent temperature and daily number of deaths for 15 European cities during the hot period (assumed to be between 1st April and 30th September), found that, above a threshold of 29.4 °C for Mediterranean cities and 23.3 °C for north-continental ones, an exponentially increasing excess of risk of death starts to take place. Similar studies performed in U.S. [14] have found a similar relationship between temperature and excess risk of mortality, with thresholds variable between about 23°C and about 26°C. Moreover, a study performed by Tan et al.[15], examining 30

years of meteorological data for Shanghai has demonstrated an almost linear relationship between UHI intensity and excess mortality rate.

UHI has an enormous impact on the energy consumption of buildings. Studies performed by Santamouris et al. [17] have found that cooling energy demand of a typical office buildings located in the central area of Athens is almost two times higher than the one of a similar building located in suburban areas, with peak electricity loads almost tripled. Moreover, existing studies correlating the energy consumptions of similar buildings located in urban and rural areas have revealed an average increase of the cooling load of about 13%, with an annual global energy penalty for unit of city surface and degree of UHI intensity of 0.74 kWh·m-2·K-1 [18].

Therefore, future roadmap of developments of the building sector have to take into account measures to mitigate the effects of UHI and, therefore, decrease energy demand of building stock and eradicating the energy poverty [9]. Urban climate mitigation technologies and techniques [19] have already been applied in more than 200 real scale projects, with an average temperature drop of 2 °C [20].

The aim of this paper is to explore the benefits of mitigation strategies involving the use of cool pavements, streets and roof, and the use of greenery for outdoor pavements and roofs on the reduction of outdoor peak ambient temperature and of the building energy demand. Metropolitan Sydney (NSW, Australia) was selected as an emblematic case of city affected by high UHI intensity. A detailed parametric study [21] showed that Sydney metropolitan region experiences high temperature differences within its boundaries, with a maximum difference of temperature of 6 °C. Moreover, it was demonstrated that local climate in Sydney has a high impact on cooling energy demand of buildings, with a ratio of up to 3 between Cooling Degree Days of hotter and colder spots within the region.

2. Materials and Methods

An urban zone within the neighbourhood of Chippendale, Sydney (33°53'12.03"S, 151°11'52.31"E, altitude of 20 m above sea level), was selected as case study.

The area, shown in Figure 1, represents the urban area that we decided to consider for our analyses. The area is characterized by a mixture of single family terrace houses, multi-storey medium and high density residential developments and old warehouses reconverted to residential or commercial uses. According to the latest data available from the census of population and housing conducted in 2016 [22] in the neighbourhood of Chippendale 98.4% of dwellings are medium or high density, compared to 96% in the City of Sydney, and therefore we can conclude that the selected area well represents the typical pattern of a compact urban site in Sydney's central area. The area's extension is of about 700 m in the east-west direction and about 450 m in the north-south one. The boundaries of the area are represented by two heavy-traffic roads on the north-south direction: Broadway on north and Cleveland street on south, while the east bound is represented by a heavy-traffic road – Regent street – which separates the neighbourhood from a major railway path, and the west bound is represented by a heavy-traffic road – City Road – which separates the neighbourhood from Victoria park.



Figure 1. Aerial image of the selected area

Table 1 includes the details of proposed mitigation scenarios, which have been applied to the selected urban area. The main parameters are the albedo (global or local applied to streets, outdoor pavements, or roofs) with a range of variability between a minimum of 0.1 and a maximum of 0.7, the percentage of outdoor pavements integrating greenery, with a standard value of 5% and maximum value of 60%, and the percentage of green roofs, considering the extreme cases of 0% or 100%. It has to be noted that, in our analyses, we have identified as outdoor pavements all sidewalks and buildings' parking lots. The same type of greenery was used for all areas in the ENVI-met simulations, and the type selected was Conifer Tree, 7m height.

The range of variability of albedo (global, streets, pavements, roofs) has been selected as to be representative of all possible scenarios. The highest limit (0.7) is considered to be the maximum potential and for many materials might be hindered by ageing [23-25], with phenomena that can reduce substantially and up to 50% the mitigation potential [26, 27]. Moreover, pavements and streets with too high values of Solar Reflectance (SR) are undesirable as they might cause glare [28].

Table 1. Mitigation scenarios

Category	Scenario ID	Global Albedo	Albedo Streets	Albedo Pavements	Albedo Roofs	Greenery Pavements	Greenery Roofs
Base case	1	0.1	-	-	-	5%	-
Global Albedo	2	0.2	-	-	-	5%	-
	3	0.3	-	-	-	5%	-
	4	0.5	-	-	-	5%	-
	5	0.7	-	-	-	5%	-
Albedo Streets	6	-	0.2	0.1	0.1	5%	-
	7	-	0.3	0.1	0.1	5%	-
	8	-	0.5	0.1	0.1	5%	-
	9	-	0.7	0.1	0.1	5%	-
Albedo Pavements	10	-	0.1	0.2	0.1	5%	-
	11	-	0.1	0.3	0.1	5%	-
	12	-	0.1	0.5	0.1	5%	-
	13	-	0.1	0.7	0.1	5%	-
Albedo Roofs	14	-	0.1	0.1	0.2	5%	-
	15	-	0.1	0.1	0.3	5%	-
	16	-	0.1	0.1	0.5	5%	-
	17	-	0.1	0.1	0.7	5%	-
Greenery	18	0.1	-	-	-	20%	-
	19	0.1	-	-	-	40%	-
	20	0.1	-	-	-	60%	-
Green roofs	21	0.1	-	-	-	5%	100%

The urban area has been modelled using the ENVI-met tool [29]. ENVI-met is a software based on tri-dimensional model for the prediction of energy and water interactions between outdoor surfaces (buildings' facades and roofs, outdoor streets and pavements), air, plants and greenery [30, 31]. The model accounts for longwave and shortwave radiation fluxes, transpiration and evapotranspiration from vegetation, and air movement through an integrated Computational Fluid Dynamics (CFD) algorithm. ENVI-met has been extensively validated by comparing its results against real measurements [32-36]. Moreover, in the last decades ENVI-met has been used to predict the effects of mitigation technologies in urban environment [37], to calculate outdoor thermal comfort indexes [38], and to predict future building energy consumptions [39].

ENVI-met works with a spatial discretization range between 0.5 m and 10 m and, in the particular study here described, a spatial discretization of 3.7 m x 3.7 m was adopted for the horizontal plane, while the vertical height of the cells has been imposed equal to 2 m. The total model includes a grid of 200 x 200 x 20 cells, thus resulting in a total dimension of the modelled volume of 740 m x 740 m x 40 m. Moreover, open lateral boundary conditions were applied.

All simulations were performed for a typical day, representative of warm summer climatic conditions, identified as the 1st of January. The specific nature of the day was not considered in the simulations and, therefore, it was considered as any other working days. For the determination of the simulation start-up parameters, included in the Table 2 the Meteonorm global climate database was used [40]. The database was used instead of measured variables in order to define a statistically significant pattern of climatic variables representative of a typical summer day, while the non-forcing mode option was adopted for the determination of the hourly profile of outdoor variables. In this way the profile of the outdoor temperature was directly derived from the initial air temperature and from the solar radiation calculated by the software as a function of input values of latitude and longitude of the site. In order to account for the dynamic effect given by the thermal inertia of the soil and greenery, and the effects of buildings and outdoor pavements, each simulation has been carried out for a full 25-hours cycle (starting at 0:00 and ending at 24:00). While the model includes the thermal inertia of soil and greenery, heat storage from building is not simulated. Hence, the 25-hours cycle has been considered as appropriate in order to balance computational time and precision of the outputs.

114 *Table 2. Set-up parameters for 1st January in Sydney (NSW, Australia).*

Parameter	value
Wind speed at 10m above ground	3.8 m/s
Wind direction	173°
Roughness length at reference point	0.6 m
Initial temperature atmosphere	23.9 °C
Specific humidity in 2500 m	7 g water/kg air
Relative humidity in 2 m	65%

115

116 In order to assess the decrease of cooling energy demand associated with the adoption of UHI mitigation strategies, the
117 following steps have been pursued. These are in line with studies found in literature, which couple building energy
118 simulation software with microclimate analyses performed with ENVI-met [38, 39, 41]. First, for each strategy a full one-
119 day climatic file, including 24 hourly values of all climatic variables, was created using the results of the ENVI-met
120 models. The climatic file includes the simulated values of ambient temperature and relative humidity (both calculated at
121 2 m above the ground), and wind speed (calculated at 10 m above the ground). Then the developed climatic files were
122 used as input for the simulation of the cooling load for a typical building. Simulations have been performed for a period
123 of 10 consecutive days with the same characteristics. Given the characteristics of the area and the prevailing typology, a
124 residential building was selected as typical building. The specific model selected was the Mid-Rise Apartment Reference
125 Building, developed by the U.S. Department of Energy (D.O.E.). The model is representative of a multifamily residential
126 building of 4 storeys of height. It is constituted of 32 conditioned thermal zones (31 apartments and 1 office), and 4
127 unconditioned thermal zones (corridors), for a total internal area of 3135 m2 [42]. With regards to this model, cooling
128 and heating loads were calculated for the whole day considering an Ideal Loads Air System using the software EnergyPlus
129 [43]. This module allows to define the heating and cooling loads in ideal conditions, i.e. without modelling the full
130 Heating, Ventilation and Air Conditioning (HVAC) system and considering an infinite heating and cooling capacity of
131 the system. In this way, it is possible to exclude the differences in the cooling and heating load due to the specific sizing
132 of the same HVAC system subject to different boundary conditions.

3. Results and discussion

3.1. Effects of mitigation technologies on peak ambient temperature

The effects of mitigation scenarios summarized in Table 1, simulated by means of ENVI-Met software are reported in the following figures. In particular, in this paragraph, are shown the results of ambient temperature variations, recorded at 2 pm at a height of 2 m above ground.

As summarized in Figure 2, in the base case scenario, the maximum temperature recorded at 2 pm in the typical summer day varies between 25.5°C and 28.5°C, with an average ambient temperature close to 27.5°C. Minimum values of temperature have been recorded in large open spaces and in streets with east-west orientation, which are shaded by surrounding buildings. While, on the contrary, the highest temperature values have been recorded for narrow paved streets with north-south orientation.

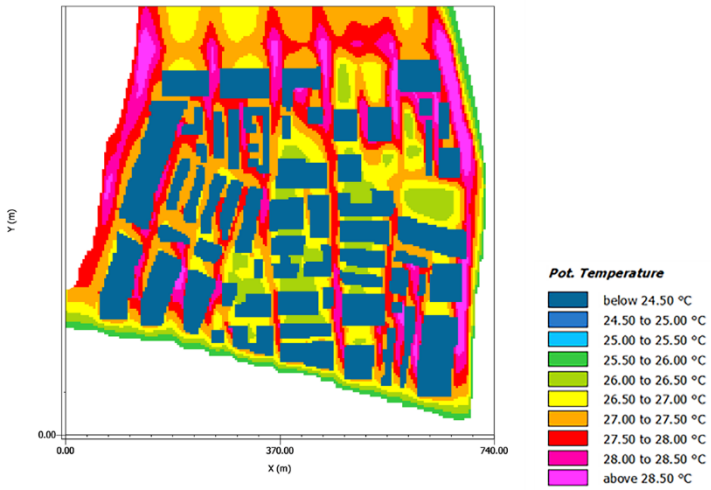


Figure 2. Temperature distribution at the ground level of base case scenario (ID 1)

From the analysis of wind patterns summarized in Figure 3, in most of the cases wind speed is lower than 3.8 m/s, which is the wind speed imposed at the boundary, except for narrow streets with north-south exposure, where limited urban canyon effects are determined.

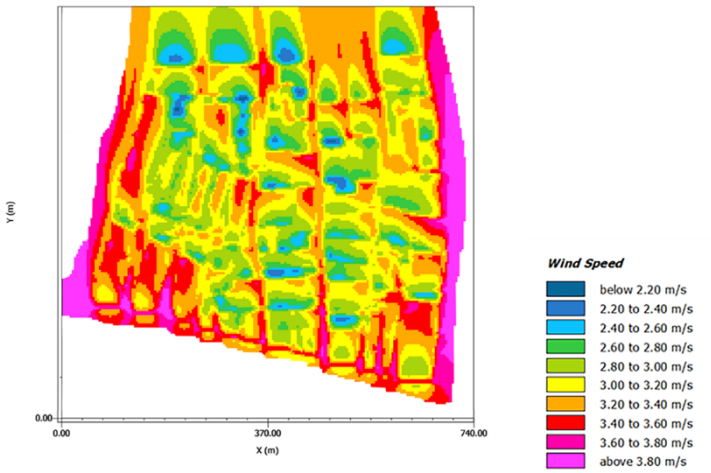


Figure 3. Wind speed distribution at the ground level of base case scenario (ID 1)

The first mitigation strategy assessed dealt with the increase of the global albedo (i.e. average solar reflectivity of all outdoor surfaces: roofs, pavements and streets), with an assigned variability between 0.2 and 0.7. Figure 4 summarizes

the results of the predictions of change in ambient temperature at 2 pm. The results indicate that for an increase of the global albedo between 0.1 and 0.6, the maximum ambient temperature is expected to decrease by 0.6 °C and 3 °C respectively. From the analysis of the abovementioned figure, it is also evident that horizontal gradients of air temperature within the area tend to decrease with the increase of the global albedo.

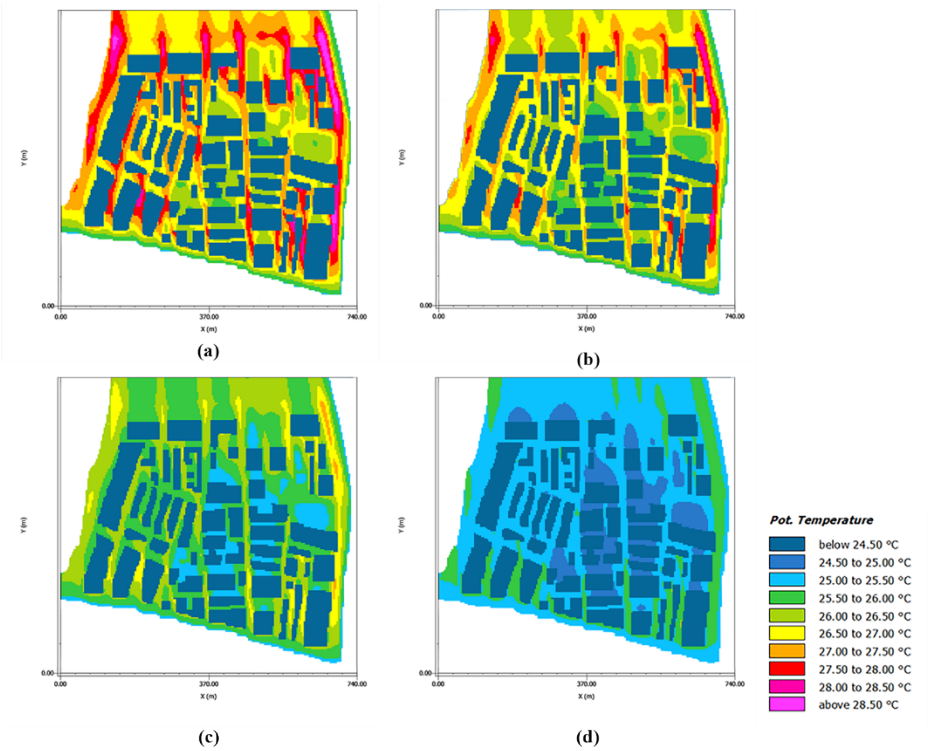


Figure 4. Temperature distribution at the ground level of scenarios involving the increase of the global albedo. (a) Scenario ID 2; (b) Scenario ID 3; (c) Scenario ID 4; (d) Scenario ID 5.

Within the strategy involving the increase of global albedo, the three cases of selective increase of the albedo for the streets, pavements and roofs have been analysed in detail, so as to understand the sensitivity of the model to the three strategies.

Figure 5 shows the results of predictions of ambient temperature in case of a selective increase of the albedo of streets from 0.1 to 0.6. The results show a potential decrease of the maximum temperature in the range between 0.4 °C and 1.4 °C. Moreover, the reduction of maximum air temperature is almost in linear relationship with the increase of the albedo and benefits are higher in narrow street north-south oriented than in street with east-west orientation which are affected by a higher shading from surrounding buildings.

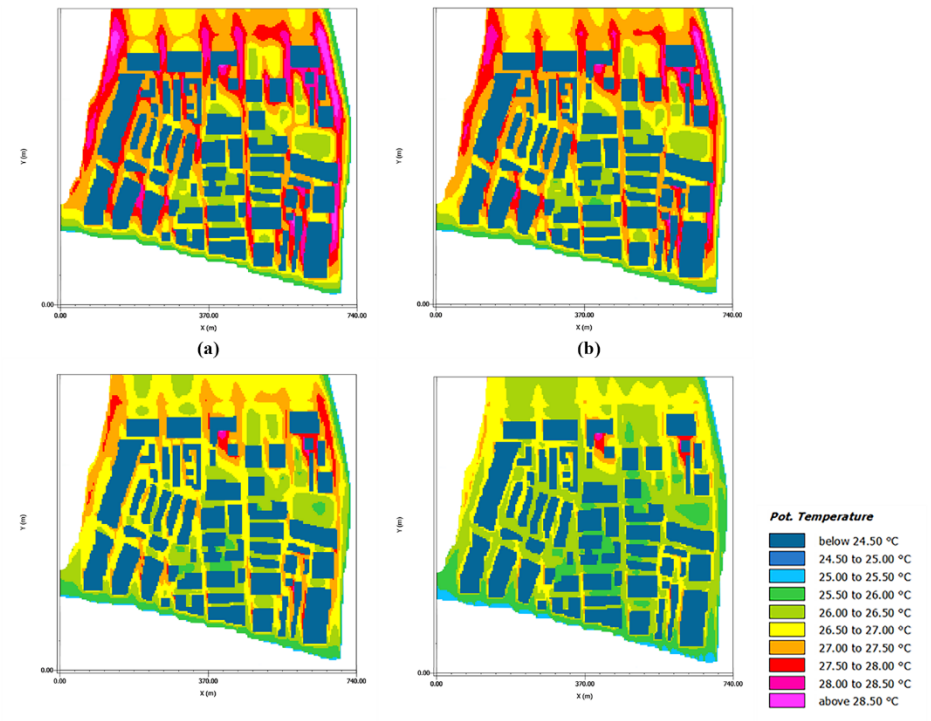


Figure 5. Temperature distribution at the ground level of scenarios involving the increase of the albedo of streets. (a) Scenario ID 6; (b) Scenario ID 7; (c) Scenario ID 8; (d) Scenario ID 9.

Predictions of air temperature reduction due to the implementation of outdoor pavements with high albedo are included in Figure 6. In this case, in comparison with the previous scenarios, results are less remarkable, with a maximum reduction of the air temperature of about 0.5 °C, due to the smaller extent of outdoor pavements in comparison to streets.

Figure 7 includes results of mitigation strategies applied to roofs. In particular, the figure shows the change in the air temperature profile at ground level when claddings with SR of 0.2, 0.4, 0.5, and 0.7 are applied on all roofs of buildings within the selected area. As for the previous case, the maximum reduction of peak ambient temperature at ground level is relatively low and in the range between 0.1 °C and 0.6 °C.

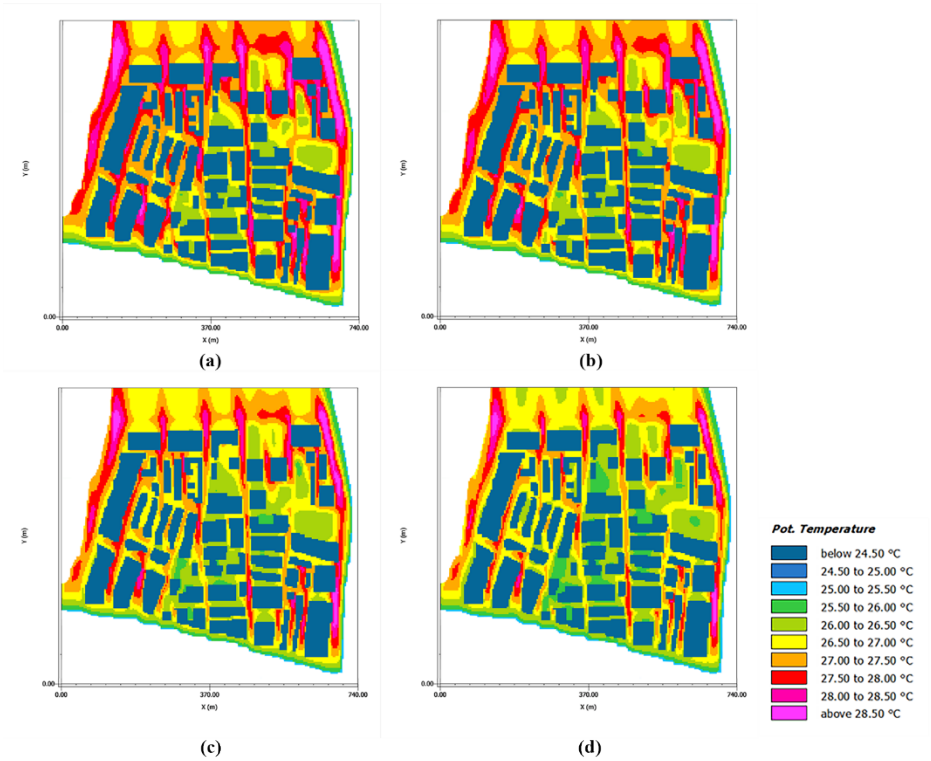


Figure 6. Temperature distribution at the ground level of scenarios involving the increase of the albedo of pavements. (a) Scenario ID 10; (b) Scenario ID 11; (c) Scenario ID 12; (d) Scenario ID 13.

Finally, by increasing the amount of greenery coverage in the area to respectively 20%, 40%, and 60% of total ground area in comparison with the 5% used in the base case scenario, a decrease of peak air temperature between 0.3 °C and 1.4 °C has been predicted. Moreover, by introducing greenery on all roofs a decrease of peak ambient temperature close to 0.5 °C has been calculated, as shown in Figure 8 (d). These results are, indeed, in line with all the other strategies involving interventions on roof, which seem not to be highly effective in reducing the ambient temperature at ground level in comparison with strategies involving the increase of global albedo.

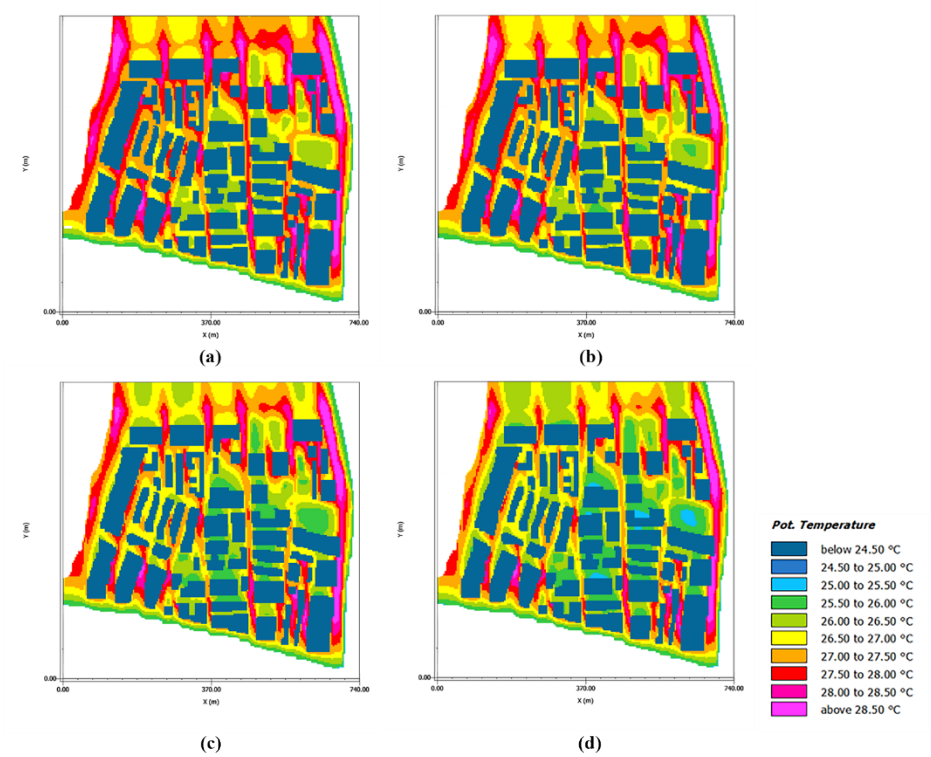


Figure 7. Temperature distribution at the ground level of scenarios involving the increase of the albedo of roofs. (a) Scenario ID 14; (b) Scenario ID 15; (c) Scenario ID 16; (d) Scenario ID 17.

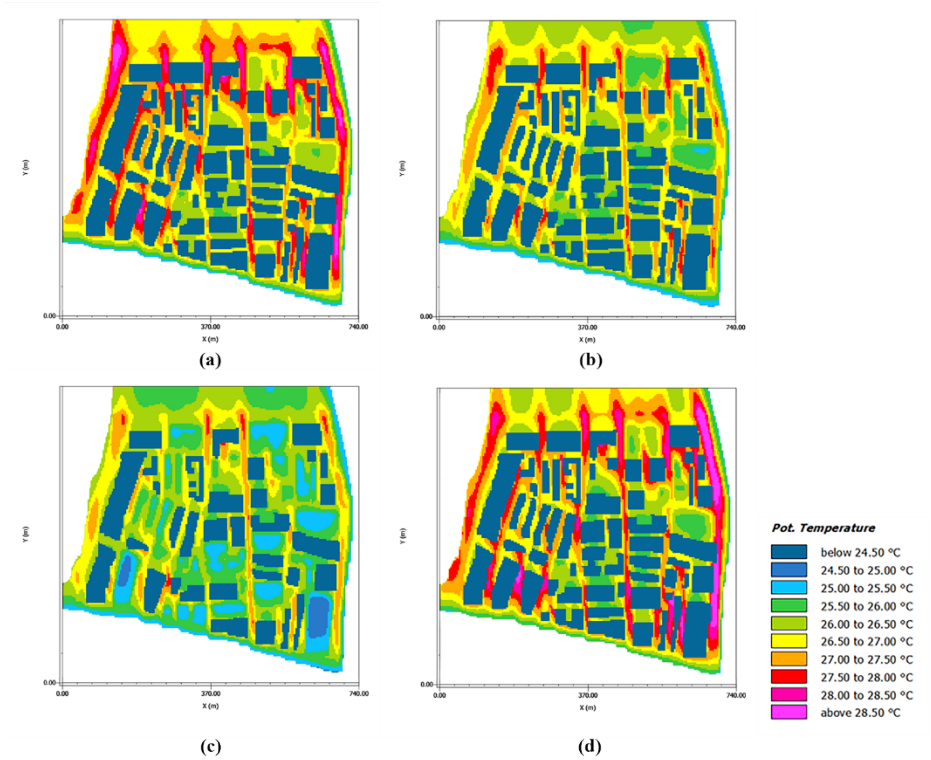


Figure 8. Temperature distribution at the ground level of scenarios involving the increase of the greenery. (a) Increase of the greenery at ground level to 20% (ID 18); (b) Increase of the greenery at ground level to 40% (ID 19); (c) Increase of the greenery at ground level to 60% (ID 20); (d) Implementation of green roofs on the 100% of the area (ID 21).

Overall simulations have shown that the possible mitigation technologies might contribute to the decrease of the peak ambient temperature of up to 3 °C, even though experimental results based on in-field measurements in similar cases show that it could be more realistic to consider that the application of the mitigation technologies described before might

contribute to the decrease of the peak ambient temperature of up to 1.5 °C [20]. However, it is important to highlight that by simulating scenarios involving different mitigation technologies can help in understanding the relative benefit of each technology. Moreover, the results of ENVI-met analyses have been helpful in creating modified weather scenarios essential for performing significant prediction of building energy demand, as described in the following paragraph.

3.2. Effects of mitigation technologies on cooling loads

As previously described, ENVI-met simulations have been coupled with an EnergyPlus model to define the effects of mitigation technologies on the maximum cooling load of a typical residential building. Hourly values of outdoor microclimatic variables have been obtained as output from ENVI-met software and used to generate a new input weather file for EnergyPlus. The input weather file consisted of 10 identical consecutive days. As previously described, this activity has been performed to predict the impacts of mitigation technology, including both direct (i.e. modification of SR or thermal properties of roofs) and indirect effects due to the modification of outdoor microclimatic variables as a result of the application of the mitigation technology.

Table 3 includes a summary of the calculated cooling loads during the 10 days of simulations performed on the typical residential building. The cooling loads range from 2.35 kWh/m2 (i.e. 0.235 kWh/m2 day) for the base case scenario, down to 1.89 kWh/m2 (i.e. 0.189 kWh/m2 day) for scenario 5, in which outdoor surfaces with global albedo of 0.7 are considered. Scenario 5 represents the best mitigation solution for the reduction of building cooling demand among the 21 scenarios modelled.

Table 3. Calculated cooling loads for the typical building under the 21 scenarios.

Category	Scenario ID	Cooling load [kWh/m2]	Energy conservation [%]
Base case	1	2.35	
Global Albedo	2	2.28	-3.00 %
	3	2.21	-6.00 %
	4	1.94	-17.00 %
	5	1.89	-20.00 %
Albedo Streets	6	2.34	-0.11 %
	7	2.34	-0.46 %
	8	2.32	-0.97 %
	9	2.31	-1.54 %
Albedo Pavements	10	2.34	-0.36 %
	11	2.34	-0.20 %
	12	2.31	-1.65 %
	13	2.29	-2.42 %
Albedo Roofs	14	2.30	-2.10 %
	15	2.24	-4.62 %
	16	1.90	-18.98 %
	17	1.90	-19.06 %
Greenery	18	2.34	-0.48 %
	19	2.32	-1.23 %
	20	2.29	-2.31 %
Green roofs	21	2.35	+0.2 %

By the detailed analysis of the results, it can be highlighted that for the examined case the most effective strategies are the ones involving the adoption of high-albedo surfaces. As a matter of fact, the global increase of the albedo produces a reduction of peak cooling demand of residential buildings of 20% when the global albedo is increased from 0.1 to 0.7. Among this strategy, the increase of the albedo of roofs has the highest beneficial effects on building energy demand. On average, each 0.1 of increase of SR results in a predicted saving in peak cooling load of 3.5%. The results obtained are in good agreement with existing literature and in particular with studies reporting experimental analyses carried out in similar climates (i.e. Koppen-Geiger climate C – warm temperate). Parker & Barkaszi [44] performed an experimental

campaign involving measurements of daily and peak energy demand on 8 residential buildings in Florida (U.S.A.) before and after the application of a high-albedo coating on the roof cladding. They found that by increasing the roof's SR by 0.3-0.53 an average daily saving of energy between 2% and 43% was measured, while the peak energy saving was reduced by a percentage variable between 12% and 28%. Miller et al. [45] reported the final results of a research project involving monitoring of several demonstration homes in California (U.S.A.) in which cool concrete tile roofs (SR 0.41) and cool painted metal roofs (SR 0.31) were installed. Results were, then, compared with monitoring of houses of the same typology in which traditional concrete roofs (SR 0.10) and metal roofs were installed (SR 0.08). They did find an average saving of 9% for the buildings equipped with concrete tile roofs and of 8 to 10% for the ones equipped with cool painted metal roofs. A similar study was performed by Rosado et al. [46], who measured temperature, heat flows and energy use of two single-storey residential buildings with asphalt shingle roof (SR 0.07) and cool concrete tile one (SR 0.51) and found an annual cooling energy saving of 26% due to the use of the cool roof technology. Kolokotroni et al. [47] performed an experimental study of an office building and predicted, by means of TRNSYS modelling, a reduction of the cooling demand of 17.44% when the traditional roof cladding (SR 0.1) was substituted with a cool one (SR 0.6).

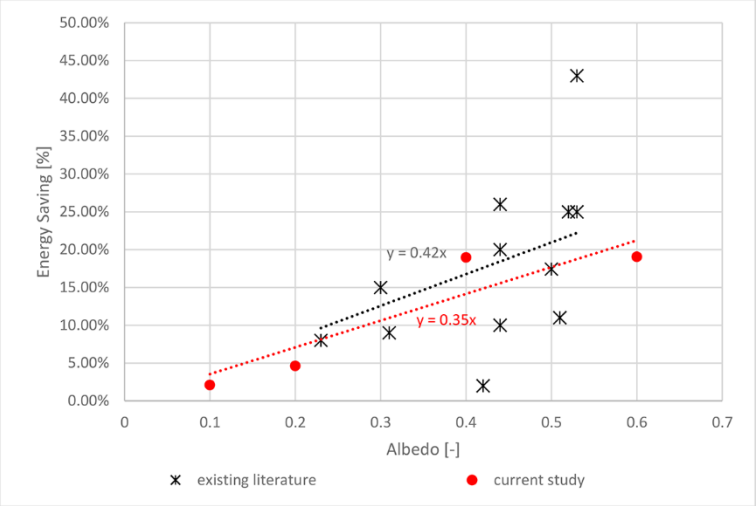


Figure 9: comparison of energy savings due to the use of cool roofs with results of experiments reported in literature [44-47]

Overall, for the case of cool roofs, by comparing the results of our predictions with existing experiments reported in literature, it can be found a good agreement between the two sets of data. Figure 9 shows a comparison of the relationship between expected energy savings and increase of roofs' albedo obtained from our simulations (designated in the graph with red dots), and the same relationship based on information reported in literature (designated in the graph with black crosses). The two regression lines show a similar behaviour and almost the same slope. In particular in our findings each 0.1 increase of SR results in a reduction of cooling energy demand of 3.5%, very close to the 4.2% saving reported in literature. However, it has to be highlighted that data reported in literature have a higher variance than the ones calculated by us, especially when increase of albedo of more than 40% is analysed, with calculated energy saving for reduction of cooling load ranging from 2% to 43%. It has to be noted that most of the experiments reported in literature examine just the direct impact of cool roofs on building energy demand, while in our case the benefit of accounting for indirect impacts is added.

Less beneficial, but still with remarkable energy savings, are the two strategies involving respectively the increase of the albedo of streets and outdoor pavements, with reductions of about 0.04% and 0.025% of cooling energy demand for each 10% of albedo increase. As also pointed out by Gilbert et al. [48], in temperate and hot areas the energy saving obtained by the adoption of cool pavements is of an order of magnitude smaller than the equivalent saving achieved by means of the adoption of cool roofs.

Figure 10 includes the overall comparison of benefits of all mitigation strategies involving the increase of albedo (global, of roofs, of pavement, and of streets). The graph shows the relationship between increase of albedo, with reference to the base case, and expected energy saving due to the reduction of cooling energy demand. All the strategies show with a good approximation an almost linear relationship between the increase of the albedo and the expected energy savings for cooling, confirmed by coefficients of determination higher than 0.9 for all regression lines. The strategies involving the increase of the global albedo (represented in the figure with blue circles) and the increase of the albedo of roofs (represented in the figure with black squares) show comparable results, with a maximum energy saving, of about 20%, when the albedo is increased by 0.6 and a minimum value of expected energy saving, of about 2-3%, when the albedo is increased of 0.1. Overall the two regression lines are almost coincident and, as an average, each 10% of increase of albedo produces an energy saving benefit of about 3.5%. On the contrary, strategies concentrated on horizontal surfaces at the ground level, involving the increase of albedo of outdoor pavements (grey triangles in the figure) and of streets (red rhombuses in the figure) show maximum benefits in the order of 1.5-2.5% when the albedo is increased by 0.6. Both strategies show energy benefits of one order of magnitude lower than the ones obtained from the adoption of the previous two strategies and, as an average, each 10% increase of albedo of streets or of outdoor pavements results in a reduction of cooling energy demand between 0.2% and 0.4%.

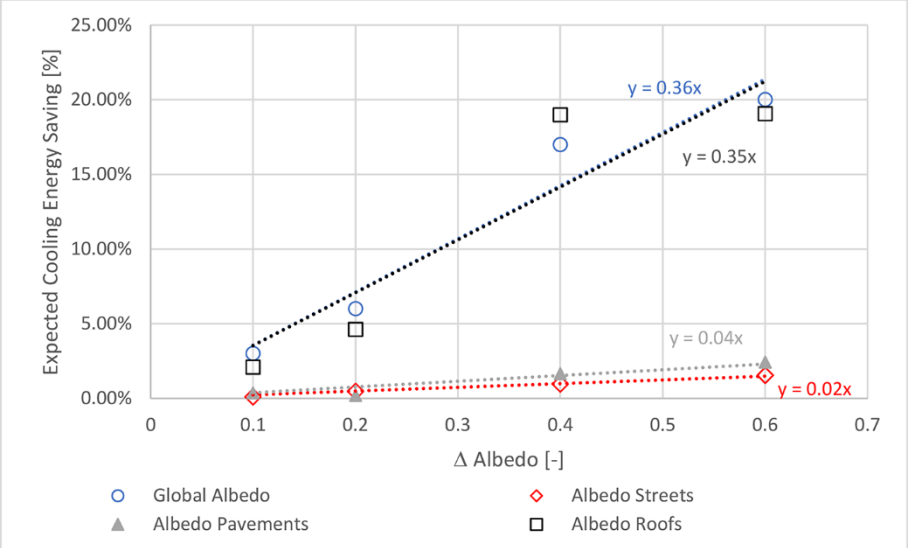


Figure 10. Variation of expected energy savings because of the increase of albedo

Table 3 includes also the results of expected energy saving due to the reduction of cooling loads when strategies involving the use of greenery are adopted. In line with what has already been depicted from the analysis of the graphs of peak ambient temperature the increase in percentage of outdoor green areas produces limited benefits on the reduction of building cooling demand. However, these results are in line with those of other mitigation strategies focused on outdoor pavements and streets. Also in the case, the reduction of cooling energy demand is in an almost linear relationship with the percentage of outdoor area covered with greenery. A maximum reduction of cooling load of about 2.3% was achieved with additional greenery on the 55% of the outdoor area and, as an average, each 10% of additional greenery on outdoor spaces produces a potential decrease of the cooling energy demand of about 0.4%.

Finally, the strategy involving the use of green roofs is not so beneficial under an energy point of view, as the implementation of greenery on the roof of residential buildings in Sydney creates no benefit under a cooling load point of view, presenting cooling peak demand very close to the one of the base case scenario. The reasons for these results can be found by analysing the results included in literature on the cooling energy demand of residential buildings equipped with green roofs. Several studies performed in Mediterranean areas found a decrease of about 10% of the cooling energy

demand of building equipped with green roofs in comparison with the equivalent ones with traditional roofs. Sfakianaki et al. [49] performed a theoretical and experimental analysis of the benefits of green roofs in residential buildings in Athens, Greece. They did find that in buildings equipped with green roofs the cooling energy demand was about 11% lower than the one of buildings with conventional bare roofs. Jaffal et al. [50] found that, for a residential single-storey building located in La Rochelle, the implementation of green roofs determines a reduction of annual cooling load of 2.3-2.4 kWh/m2 with respect to conventional roofs. Zinzi and Agnoli [51] carried out a perspective assessment on the energy benefits of mitigation technologies applied to residential buildings in the Mediterranean area. They did find a reduction of cooling energy demand up to 10% when green roofs are installed instead of conventional ones.

In our study, on the contrary, we did find that no reduction of cooling demand during the selected day was achieved when green roofs were substituted to existing ones. In our opinion there are several concurrent reasons for this result. Firstly, the results are highly affected by the specific typology of building selected. As a matter of fact, we concentrated on a medium-size building of 4 storeys of height, in which the relative benefits of green roofs on the cooling load of the entire building is limited. On the contrary all the previous research concentrate on buildings of lower height were the effect of green roofs could be relevant. The second factor affecting the results is the level of insulation. As demonstrated by Silva et al. [52], for extensive green roofs, the increase of insulation levels determines an increase of the cooling energy demand in comparison with the one of a building with conventional roofs and the same level of roof insulation. In our analyses, having adopted a solution with medium/high level of insulation, we did find similar results. Thirdly, it can be argued that the reduction of cooling load can be influenced by the reduction of ambient temperature that cool roofs contribute to achieve; in our analyses we did find a reduction of about 0.5 °C of peak ambient temperature and, therefore, lower levels of reduction of cooling energy demand were expected in comparison with the ones achieved by the adoption of other strategies. Overall it can be concluded that the benefits of this technology have to be assessed not only during hot season, but during the entire year, as the decrease of heating load could compensate the increase of cooling loads.

Conclusions

Metropolitan Sydney is highly affected by UHI phenomenon, with maximum recorded gradient of peak ambient temperature of 6 °C. This circumstance highly affects the liveability of the denser portions of the city and buildings energy demand, with an increase of up to three times of the cooling degree days between hotter and colder spots within the area. Mitigation technologies applied to a central area of Sydney have demonstrated to be beneficial in reducing peak ambient temperatures.

Overall the results have indicated that:

- Strategies involving the increase of global albedo in the city are the most effective in reducing peak ambient temperature, with a decrease between 0.3 °C and 3 °C when global albedo is increased between 0.1 and 0.6.
- Strategies involving interventions on outdoor areas, either increasing the albedo of streets, or increasing the percentage of outdoor greenery help in reducing the peak ambient temperature from 0.3°C to 1.4 °C.
- Mitigation interventions on roofs (either through the increase of their albedo or through the implementation of green roofs) do not contribute significantly to the reduction of peak ambient temperature at ground level, with a maximum calculated decrease of about 0.5 °C. However, they are among the strategies with the highest benefits in minimizing the peak cooling loads of the buildings.

Urban climate simulations, coupled with a detailed thermal dynamic analysis of a typical residential building have contributed to the definition of potential energy savings due to the adoption of the above-mentioned mitigation technologies.

Analysing the results of thermal dynamic simulations, it can be concluded that:

- The increase of global albedo and the increase of albedo of roofs have demonstrated to be highly effective strategies under an energy saving point of view, with a predicted decrease of peak cooling load of respectively 3.6% and 3.5% for each 10% of increase of the albedo.
- Strategies involving the increase of the albedo of outdoor horizontal surfaces at ground level (pavements and streets) show benefits of one order or magnitude lower than the one of the previous scenario, with an expected decrease of the peak cooling load of respectively 0.4% and 0.2% for each 10% of increase of the albedo. Comparable results have been obtained by increasing greenery on outdoor spaces: each 10% of increase of outdoor greenery contributes to the reduction of peak cooling load of buildings of 0.4%.
- Mitigation solutions involving the use of greenery on roofs have demonstrated to be not so beneficial in reducing building cooling demand. However, their benefit has to be assessed with an analysis extended to the entire year as the decrease of heating loads largely compensates a small increase of cooling loads.

Overall, it can be concluded that, through a combined analysis involving microclimatic modelling and energy simulations we have been able to assess the simultaneous benefits of mitigation technologies under both an energy and an environmental point of view. The results could be helpful in obtaining a screening of the mitigation technologies to be adopted in a selected area with the aim of selecting the ones to be designed, implemented and tested. Finally, the workflow that we have been elaborated could be effectively adopted in other urban sites in order to provide support to the decision-making process on UHI mitigation strategies to be implemented.

Acknowledgements

The research activities described in the current paper have been funded through the SJTU-UNSW Collaborative Research Fund – Seed Grant RG152786.

Author Contributions

M. Santamouris conceived and designed the experiments; M. Saliari performed the simulations; F. Fiorito analysed the data and wrote the paper; all authors contributed to the editing of the paper.

Conflicts of Interest

The authors declare no conflict of interest.

References

[1] T.R. Oke, City size and the urban heat island, Atmospheric Environment (1967), 7 (8) (1973) 769-779.
[2] T.R. Oke, Canyon geometry and the nocturnal urban heat island: Comparison of scale model and field observations, Journal of Climatology, 1 (3) (1981) 237-254.
[3] H.E. Landsberg, The urban climate, The urban climate., (1982).
[4] T.R. Oke, The energetic basis of the urban heat island, Quarterly Journal of the Royal Meteorological Society, 108 (455) (1982) 1-24.
[5] H. Taha, Urban climates and heat islands: Albedo, evapotranspiration, and anthropogenic heat, Energy and Buildings, 25 (2) (1997) 99-103.
[6] A.J. Arnfield, Two decades of urban climate research: A review of turbulence, exchanges of energy and water, and the urban heat island, International Journal of Climatology, 23 (1) (2003) 1-26.
[7] M.P. McCarthy, M.J. Best, R.A. Betts, Climate change in cities due to global warming and urban effects, Geophysical Research Letters, 37 (9) (2010).

[8] M. Santamouris, Heat island research in Europe: The state of the art, Adv. Build. Energy Res., 1 (1) (2007) 123-150.
[9] M. Santamouris, Innovating to zero the building sector in Europe: Minimising the energy consumption, eradication of the energy poverty and mitigating the local climate change, Solar Energy, 128 (2016) 61-94.
[10] M. Santamouris, Analyzing the heat island magnitude and characteristics in one hundred Asian and Australian cities and regions, Science of the Total Environment, 512-513 (2015) 582-598.
[11] C. Sarrat, A. Lemonsu, V. Masson, D. Guedalia, Impact of urban heat island on regional atmospheric pollution, Atmospheric Environment, 40 (10) (2006) 1743-1758.
[12] M. Baccini, A. Biggeri, G. Accetta, T. Kosatsky, K. Katsouyanni, A. Analitis, H.R. Anderson, L. Bisanti, D. D'Ippoliti, J. Danova, B. Forsberg, S. Medina, A. Paldy, D. Rabczenko, C. Schindler, P. Michelozzi, Heat effects on mortality in 15 European cities, Epidemiology, 19 (5) (2008) 711-719.
[13] G. Luber, M. McGeehin, Climate Change and Extreme Heat Events, American Journal of Preventive Medicine, 35 (5) (2008) 429-435.
[14] M.S. O'Neill, K.L. Ebi, Temperature extremes and health: Impacts of climate variability and change in the United States, Journal of Occupational and Environmental Medicine, 51 (1) (2009) 13-25.
[15] J. Tan, Y. Zheng, X. Tang, C. Guo, L. Li, G. Song, X. Zhen, D. Yuan, A.J. Kalkstein, F. Li, H. Chen, The urban heat island and its impact on heat waves and human health in Shanghai, International Journal of Biometeorology, 54 (1) (2010) 75-84.
[16] C. Sarkar, C. Webster, Urban environments and human health: current trends and future directions, Current Opinion in Environmental Sustainability, 25 (2017) 33-44.
[17] M. Santamouris, N. Papanikolaou, I. Livada, I. Koronakis, C. Georgakis, A. Argiriou, D.N. Assimakopoulos, On the impact of urban climate on the energy consuption of building, Solar Energy, 70 (3) (2001) 201-216.
[18] M. Santamouris, On the energy impact of urban heat island and global warming on buildings, Energy and Buildings, 82 (2014) 100-113.
[19] M. Santamouris, D. Kolokotsa, Urban Climate Mitigation Techniques, Taylor & Francis, 2016.
[20] M. Santamouris, L. Ding, F. Fiorito, P. Oldfield, P. Osmond, R. Paolini, D. Prasad, A. Synnefa, Passive and active cooling for the outdoor built environment – Analysis and assessment of the cooling potential of mitigation technologies using performance data from 220 large scale projects, Solar Energy, 154 (2017) 14-33.
[21] M. Santamouris, S. Haddad, F. Fiorito, P. Osmond, L. Ding, D. Prasad, X. Zhai, R. Wang, Urban heat island and overheating characteristics in Sydney, Australia. An analysis of multiyear measurements, Sustainability (Switzerland), 9 (5) (2017).
[22] City of Sydney, .id communities demographic resources, in, https://profile.id.com.au/sydney, 2018.
[23] R. Levinson, H. Akbari, Effects of composition and exposure on the solar reflectance of portland cement concrete, Cement and Concrete Research, 32 (11) (2002) 1679-1698.
[24] N.L. Alchapar, E.N. Correa, M.A. Canton, Solar reflectance index of pedestrian pavements and their response to aging, JClean Energy Technol, 1 (4) (2013) 281-285.
[25] S. Sen, J. Roesler, Aging albedo model for asphalt pavement surfaces, Journal of Cleaner Production, 117 (Supplement C) (2016) 169-175.
[26] G.E. Kyriakodis, M. Santamouris, Using reflective pavements to mitigate urban heat island in warm climates - Results from a large scale urban mitigation project, Urban Climate, (2017).
[27] V. Lontorfos, C. Efthymiou, M. Santamouris, On the time varying mitigation performance of reflective geoengineering technologies in cities, Renew. Energy, 115 (Supplement C) (2018) 926-930.

[28] M. Santamouris, N. Gaitani, A. Spanou, M. Saliari, K. Giannopoulou, K. Vasilakopoulou, T. Kardomateas, Using cool paving materials to improve microclimate of urban areas – Design realization and results of the flisvos project, Building and Environment, 53 (Supplement C) (2012) 128-136.
[29] ENVI-met 4.2, in, www.ENVI-met.com, 2017.
[30] M. Bruse, H. Fleer, Simulating surface–plant–air interactions inside urban environments with a three dimensional numerical model, Environmental Modelling & Software, 13 (3) (1998) 373-384.
[31] M. Bruse, The influences of local environmental design on microclimate-development of a prognostic numerical Model ENVI-met for the simulation of Wind, temperature and humidity distribution in urban structures, Germany: University of Bochum, (1999).
[32] E.L. Krüger, F.O. Minella, F. Rasia, Impact of urban geometry on outdoor thermal comfort and air quality from field measurements in Curitiba, Brazil, Building and Environment, 46 (3) (2011) 621-634.
[33] X. Yang, L. Zhao, M. Bruse, Q. Meng, Evaluation of a microclimate model for predicting the thermal behavior of different ground surfaces, Building and Environment, 60 (Supplement C) (2013) 93-104.
[34] J.A. Acero, K. Herranz-Pascual, A comparison of thermal comfort conditions in four urban spaces by means of measurements and modelling techniques, Building and Environment, 93 (Part 2) (2015) 245-257.
[35] F. Salata, I. Golasi, R. de Lieto Vollaro, A. de Lieto Vollaro, Urban microclimate and outdoor thermal comfort. A proper procedure to fit ENVI-met simulation outputs to experimental data, Sustainable Cities and Society, 26 (Supplement C) (2016) 318-343.
[36] Y. Wang, U. Berardi, H. Akbari, Comparing the effects of urban heat island mitigation strategies for Toronto, Canada, Energy and Buildings, 114 (2016) 2-19.
[37] V. Tsilini, S. Papantoniou, D.-D. Kolokotsa, E.-A. Maria, Urban gardens as a solution to energy poverty and urban heat island, Sustainable Cities and Society, 14 (Supplement C) (2015) 323-333.
[38] K. Perini, A. Chokhachian, S. Dong, T. Auer, Modeling and simulating urban outdoor comfort: Coupling ENVI-Met and TRNSYS by grasshopper, Energy and Buildings, 152 (2017) 373-384.
[39] K. Gobakis, D. Kolokotsa, Coupling building energy simulation software with microclimatic simulation for the evaluation of the impact of urban outdoor conditions on the energy consumption and indoor environmental quality, Energy and Buildings, (2017).
[40] Meteotest, Meteonorm, in, http://www.meteonorm.com/.
[41] X. Yang, L. Zhao, M. Bruse, Q. Meng, An integrated simulation method for building energy performance assessment in urban environments, Energy and Buildings, 54 (Supplement C) (2012) 243-251.
[42] K. Field, M. Deru, D. Studer, Using DOE Commercial Reference Building for Simulation Studies, in: SimBuild 2010. Fourth National Conference of IBPSA-USA, New York City (USA), 2010.
[43] U.S. Department of Energy (DOE), EnergyPlus 8.6.0, in, 2016.
[44] D.S. Parker, S.F. Barkaszi, Roof solar reflectance and cooling energy use: field research results from Florida, Energy and Buildings, 25 (2) (1997) 105-115.
[45] W.A. Miller, A. Desjarlais, P. Childs, J. Atchley, H. Akbari, R. Levinson, P. Berdahl, California Home Demonstrations Showcasing the Energy Savings of Tile, Painted Metal and Asphalt Shingle Roofs with Cool Color Pigments, in, California Energy Commission. Public Interest Energy Research Program, 2006.
[46] P.J. Rosado, D. Faulkner, D.P. Sullivan, R. Levinson, Measured temperature reductions and energy savings from a cool tile roof on a central California home, Energy and Buildings, 80 (2014) 57-71.

444 [47] M. Kolokotroni, B.L. Gowreesunker, R. Giridharan, Cool roof technology in London: An experimental and
445 modelling study, Energy and Buildings, 67 (Supplement C) (2013) 658-667.
446 [48] H.E. Gilbert, P.J. Rosado, G. Ban-Weiss, J.T. Harvey, H. Li, B.H. Mandel, D. Millstein, A. Mohegh, A. Saboori,
447 R.M. Levinson, Energy and environmental consequences of a cool pavement campaign, Energy and Buildings, (2017).
448 [49] A. Sfakianaki, E. Pagalou, K. Pavou, M. Santamouris, M.N. Assimakopoulos, Theoretical and experimental analysis
449 of the thermal behaviour of a green roof system installed in two residential buildings in Athens, Greece, International
450 Journal of Energy Research, 33 (12) (2009) 1059-1069.
451 [50] I. Jaffal, S.-E. Ouldboukhitine, R. Belarbi, A comprehensive study of the impact of green roofs on building energy
452 performance, Renew. Energy, 43 (Supplement C) (2012) 157-164.
453 [51] M. Zinzi, S. Agnoli, Cool and green roofs. An energy and comfort comparison between passive cooling and
454 mitigation urban heat island techniques for residential buildings in the Mediterranean region, Energy and Buildings, 55
455 (2012) 66-76.
456 [52] C.M. Silva, M.G. Gomes, M. Silva, Green roofs energy performance in Mediterranean climate, Energy and
457 Buildings, 116 (Supplement C) (2016) 318-325.